Proceedings of the 3rd International Conference on Mathematical Physics and Computational Simulation
DOI: 10.54254/2753-8818/2025.23535

A Review on Properties, Production and Applications of Graphene

Chenrui Liang

Department of Physics, Fudan University, Shanghai, China
3510453756@qq.com

Abstract: As one of the promising two-dimensional materials in recent years, graphene has drawn considerable attention and significant progress has been made on the investigation of its supreme physical properties. This single carbonic layer shows various physical properties, like extreme mechanical strength, high electronic conductivity, unusual electronic spectrum and so on. Much more intriguing features are the shifted QHE and the commensurate-phase transition. Detailed and rigorous research is closely associated with well-prepared samples and researchers were once faced with the challenges to produce high quality wafers of graphene. All these surprising characteristics definitely provide fertile ground for the future application of graphene. Here we report the research of properties and methods of characterization of graphene and its production in laboratory in recent years and direct our attention towards several specific applications concerning photonic devices, energy storage and bio-applications.

Keywords: graphene, graphene syntheses, quantum Hall effect, commensurate-incommensurate transformation, graphene applications

1. Introduction

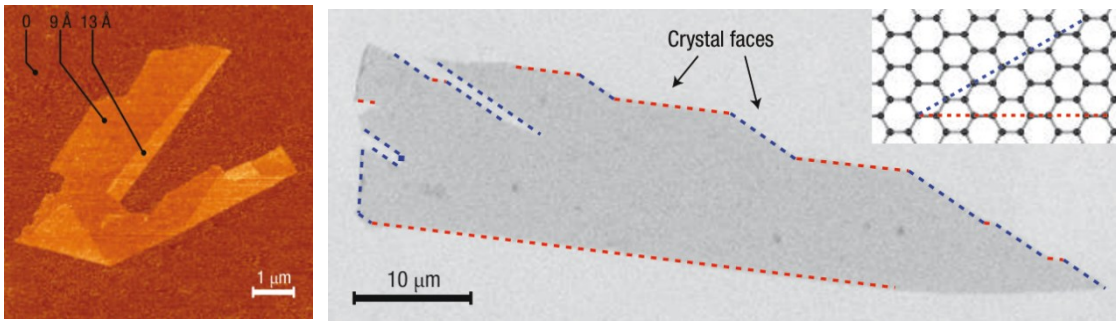

(a) (b)

Figure 1: Graphene is one of the thinnest crystals with only one atom layer.

1a: Atomic force microscopy (AFM) could be adopted to make graphene visible (adapted from [1]) so convenient for us to identify the one-atom-thick layer with a height of approximately 4 angstroms.

1b: A large wafer of graphene showing the types of edges of the crystal faces with different colored lines; these blue ones are zigzag edges while these red ones are of armchair type. (adapted from [2])

© 2025 The Authors. This is an open access article distributed under the terms of the Creative Commons Attribution License 4.0 (https://creativecommons.org/licenses/by/4.0/).

DOI: 10.54254/2753-8818/2025.23535

Graphene is a honeycomb-like single layer material constructed out of carbon atoms. With the benefit of atomic force microscopy (depicted in Figure 1a), it's easy to find the lapping area with approximate 4 angstroms height difference, indicating one-atom carbonic layer [2] and it has a 0.142 nm bond length forming one of six visualized sides of the honeycomb. Graphene exhibits two typical crystal faces: zigzag and armchair edges and they are easily visualized by scanning electron microscopy (SEM).

Its popularity can be attributed to not only supreme physical properties but also its fundamental role as building bricks for other graphitic materials with different dimensions (shown in Figure 2). Wrapping it up will create the zero-dimension buckminsterfullerene. Rolling it we get one-dimension nanotubes and stacking it we are presented with common three-dimension graphite. History studying graphene as a theoretical toy model dated back to nearly eighty years ago [3]. Nevertheless, due to the presumed instability compare with other stable forms with curving shapes, fullerenes and nanotubes for instance, it was asserted not to exist freestanding. The discovery of graphene [2][4] in the free state twenty years ago smashed the preceding assumption and lit up the enthusiasm for relevant researches.

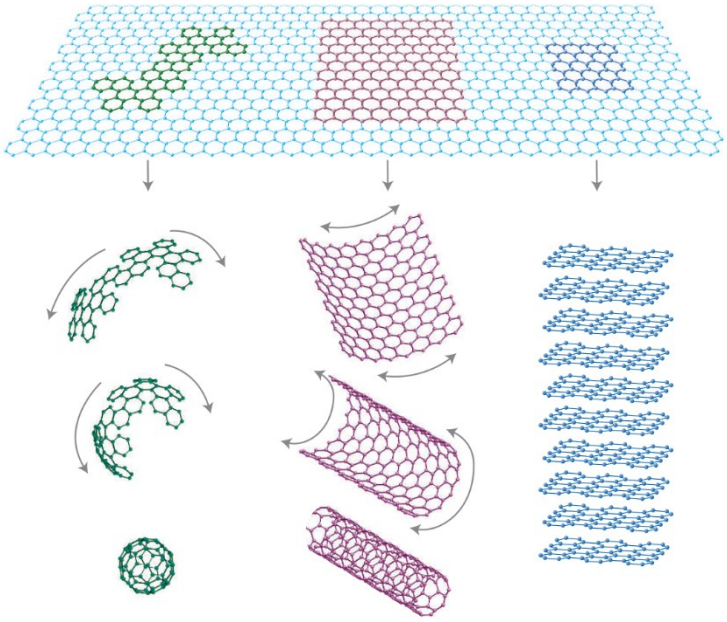

Figure 2: Building bricks for other graphitic materials. Fullerene can be obtained by wrapping up the single carbon layer and graphite originates from the stacking of graphene. (adapted from [2])

Astounding characteristics of graphene which are far superior to certain 2D materials and approaching the theory-predicted limitations include [5]: electron mobility at room temperature up to2.5×10^5; high thermal conductivities; impermeable to any gases; an extraordinarily high Young's modulus and intrinsic strength (1 TPa, 130 GPa). Unfortunately, some of the listed surprising properties are confined to samples prepared with top quality or growing on several specific substrates. Accordingly, how to obtain desired graphene samples on which rigorous investigations would be able to carry on became a great question. Here we attach the importance to two typical methods considering their contributions to different fields.

Mechanical exfoliation techniques can be used to prepare large-area graphene flakes that are high-quality. The overall scheme is to delaminate the bulk graphite into a number of thinner layers graphene with various thickness so the main obstacle confronted is find ways to surmount the attractive van der Waals forces between the adjoining layers [6]. It's very natural to adopt two

DOI: 10.54254/2753-8818/2025.23535

different approaches: one vertical and one lateral. The Nobel Prize for physics in 2004 was awarded to the micromechanical cleavage of HOPG (Highly Ordered Pyrolytic Graphite) which falls into the former category mentioned. The Scotch tape is used to apply the normal tractive force. However, the high labor-intensity and time-consumption have led to the development of experimental apparatus intended for efficiency, freeing researchers from the repeated operations in laboratory. Jayasena et al. invented a new experiment setup like a lathe to delaminate the HOPG bulk into graphene layers [7], as shown in Figure3.

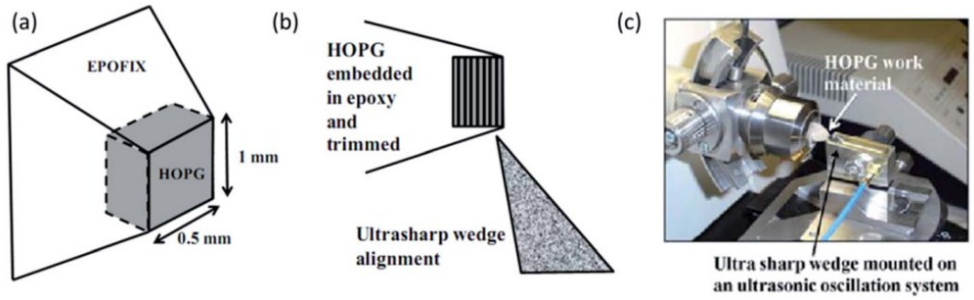

Figure 3: Manifestation of the lathe-like method for cleavage of HOPG. (adapted from [6])

3a: The epoxy pedestal is surmounted by HOPG forming the shape of a pyramid.
3b: Sharp wedge is aligned with the HOPG layers to be trimmed.
3c: The real setup for experiments.

Chemical vapor deposition (CVD), on the contrary, focuses on the scalable production of uniform graphene up to square meters flakes [8] on particular films. Defects, grain boundaries, and nonuniform thickness may appear but these films have been applied to the transparent conductive coating. One important fact deserving to be mentioned here is that the transport properties of these films on both SiO2 and hexagonal boron nitride substrates equals those of the exfoliated graphene [5] so the substrate limitations on the characteristics of graphene are not decisive. In spite of the promising application prospect, the CVD process is itself energy-consuming, let alone the need for the grown flakes to be parted from the support metal foils. Several production methods including those mentioned above have been summarized below in Figure4.

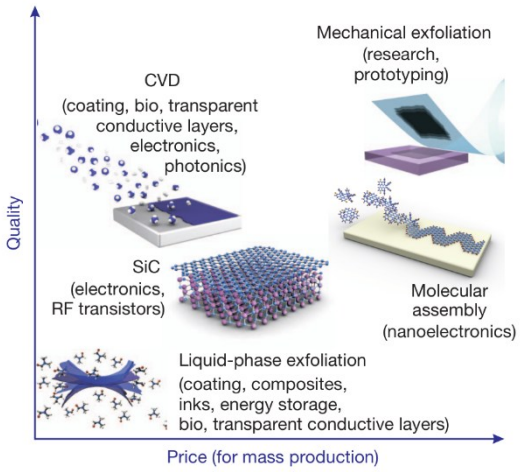

Figure 4: Various methods for large-scale graphene production. Proper balance must be kept between the price and the quality according to different production objects. (adapted from [5])

DOI: 10.54254/2753-8818/2025.23535

The preparation of single layer graphene alone is a virtual success and the visualization of graphene in an optical microscope adds luster to the achievement. Graphene placed on top of a Si film with a SiO2 coating of specific thickness (290 nm the current standard), the interference-like contrast with respect to the empty film makes it feasible for people to recognize these crystallites.[2] Quality of the graphite material and the state of the surfaces of graphene and SiO2 also play crucial part in the final results. Further detective method like Raman Spectroscopy which was found to show significant features recently, undoubtedly requires the very first capture of graphene in the optical microscope.

2. Physical properties

2.1. Quantum hall effect

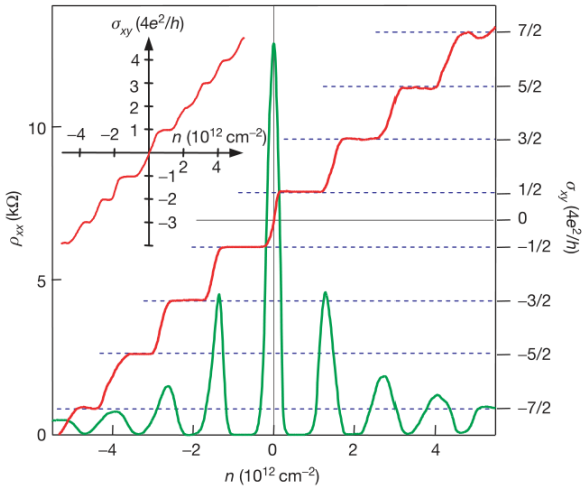

Figure 5: Quantum Hall Effect for Dirac fermions with no mass. Curves show the charge carrier concentration dependence of Hall conductivity and magnetoresistance, σ_{xy}, ρ_{xx} . Inset: Hall conductivity of a "two-layer graphene". The difference confirms that half-integer QHE is peculiar to single-layer graphene. (adopted from [10])

One of the most intriguing phenomena emerging when people are trying to understand the effects of graphene's QED-like electronic spectrum is the new quantum Hall effect (QHE). In fact, there are three kinds of QHE behaviors and we focus on one that is relativistic-like analogous to the integer QHE and typical of a single-layer graphene [9][10], depicted in Figure5. The overall structure of Hall conductivity σ_{xy} presents an ascending sequence of plateaus with equal step height. This curve persists through the Dirac point which corresponds to the neutrality of charge carriers and the sign-reversion in conductivity stands for the transition from electrons to holes. Compared with standard QHE, most striking feature of this kind is the 1/2 shift that $\sigma_{xy} = \pm\frac{4e^2}{\hbar}(N + \frac{1}{2})$ where N is the Landau level (LL).[2] This QHE is referred to as 'half-integer' in order to emphasize the shift-feature and stress its distinction between normal fractional QHE and integer QHE.

2.2. Commensurate-incommensurate transformation

Commensurate and incommensurate transformation is one attractive phenomenon which happens when a particular potential is imposed on a crystal. When it comes to heterostructures, the deposition of graphene on the hBN substrate [11] provides us with an excellent opportunity to observe such a phenomenon since the van der Waals interaction between the two surfaces plays the same role as the potential. Actually, the simulation of this transition has been performed with a classical model called

DOI: 10.54254/2753-8818/2025.23535

Frenkel-Kontorova model, in which the atoms are arranged in a chain and they are elastically linked. Due to the limitations of the materials themselves, there exist boundaries between the commensurate phases and are referred to as topological defects. Solitons are used to describe the defects in 1D while in 2D certain dislocations are adopted.

The moiré pattern of graphene and hBN can be illustrated schematically in Figure6. The period of the pattern L is negatively corelated to the misorientation angel φ between the crystallographic directions of graphene and hBN. One thing should be clarified that the existence of the pattern was ascertained by conductive and PeakForce Tapping AFM.[12]

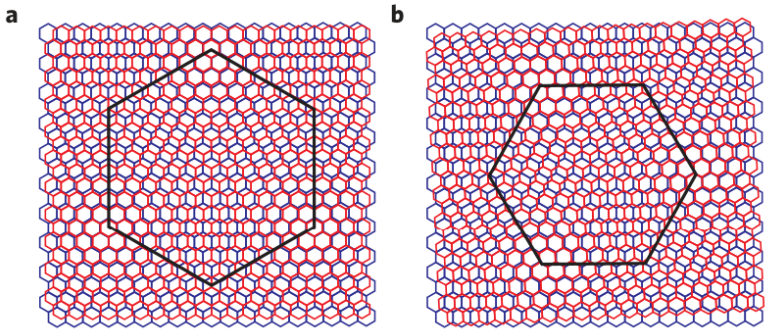

Figure 6: Visualization of the moiré pattern formed by graphene and hBN, which are represented by the red and blue honeycombs respectively. (adopted from [12])

6a: The two crystals are perfectly aligned.

6b: The misorientation angle $\varphi = 3°$. The big black hexagon represents the moiré pattern.

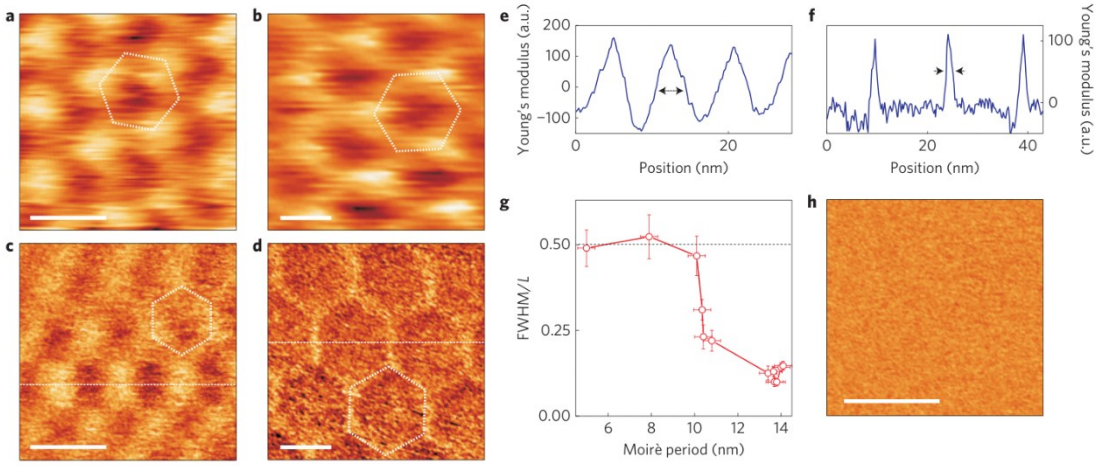

Figure 7: Observation and measurement of the moiré pattern of graphene-hBN samples with different misorientation angles. (adapted from[12])

7a, b: local resistance measured by conductive AFM for two types of samples with L=8 nm and 14 nm respectively. The deeper color corresponds to larger resistance.

7c, d: Young's modulus distribution measured in the PeakForce AFM for two types of samples with L=8 nm and 14 nm.

7e, f: Cross-section of the Young's modulus distribution measured along the dashed white lines in figure 6c and 6d respectively.

7g: Ratio of the FWHM of the peak in the cross-section Young's modulus distribution to L is plotted against L.

DOI: 10.54254/2753-8818/2025.23535

7h: Young's modulus distribution of an unaligned sample for comparison.

From the Young's modulus distributions showed in Figure 7c and 7d, it's very easy to identify the hexagonal pattern in two kinds of samples with different periods i.e. different orientation angels. The most obvious difference is the sharp contrast perceived in the kind of larger L between "the wide basins" which consists of large areas of small while basically constant Young's modulus and "the steep ridges" which represent the high peaks in value. These special terrains are much more apparent in the cross-section distribution Figure 6e and 6f. They are flattened into a sinusoidal form in samples with smaller L. All the discoveries and descriptions above are on the terms of morphology and they accord us a visualized perception of a vague transition. The reason that we regard the moiré pattern as a natural indicator of the phase transition is deeply buried in numbers. Plotting the ratio of FWHM of the peak in the distribution to L i.e. FWHM/L against L itself, we are presented with a prominent surge in the ratio (Figure 7g) thus indicating so-called commensurate-incommensurate transition.

Energy-propelled adjustment in lattice under the condition of the small rotation angel φ between the two crystals accounts for the transition to the commensurate phase, together with losses in elastic energy and gains in vdW energy [12]. If φ reaches certain critical value, the increased vdW energy is no longer able to be balanced with elastic energy so the two crystals "break up" and behave in an independent way, leading to an incommensurate phase. It's very natural to extend our imagination to the extreme case in which the vdW energy is huge enough to compensate for the negligible elastic energy in the substrate and the involved crystal would stretch or compress uniformly. However, imperfections in graphene restrain it from acting in that way, size fixed and then the nonuniformity of strain exhibits itself in the form of domains and domain walls, the former represent the commensurate area and the latter refers to the compressed regions. The analyses of the STM data of the perfectly aligned graphene-hBN samples [12] lay solid foundation for this theory because the interatomic distances in domains are larger than those in domain walls, signifying that lattices in the walls are probably compressed.

The 1D Frenkel-Kontorova model can also equip us with a compelling explanation to the transition. In this model, commensurate phases are divided by solitons and the width of soliton is formulated as $\lambda \propto \sqrt{Y/\gamma}$ where Y is the Young's modulus and γ is the depth of the background periodic potential (the minima of which is called Peierls potential). What we face here is just introduce solitons to replace a group of "screw and edge dislocations". When we rotate the two crystals away from the aligned state, the distances between dislocations decrease. At the same time, flattering of the effective Peierls potential happens and increase the width of "solitons" here i.e. dislocations. Once the angel past the critical value which is contended to be of order of the lattice mismatch, the dislocations become comparable to the moiré pattern, resulting a relatively uniformity of these misfits, different from the congregating distributions that the lattice misfits concentrate in well-defined domain walls—this stands for the commensurate-incommensurate transition.

Another significant manifestation of the difference between the two phases is the FWHM of the Raman spectrum peaks. Samples with larger moiré pattern period (L=14 nm) exhibit nearly 50% larger FWHM than these with smaller period (L=8 nm).[13] This kind of expansion can also be adopted to identify the phase transition. Let us focus on an investigation of the role annealing played in the self-rotation process [14]. Before annealing, the ratio between the width of the domain walls (δ) and the period (L) is 0.35, indicating an incommensurate phase. After annealing in a reductive atmosphere (90% Ar and 10% H2), the ratio δ/L approaches 0.2 which is a virtual herald of the commensurate phase. From Figure8 it's surprisingly easy for us to appreciate the uniform increasing in the FWHM of 2D Raman peaks almost all over the sample and shows a uniform alignment between the graphene and hBN layer. Detailed analyses point out that the misorientation angle reduces from about 1 to 0.7 degrees.

DOI: 10.54254/2753-8818/2025.23535

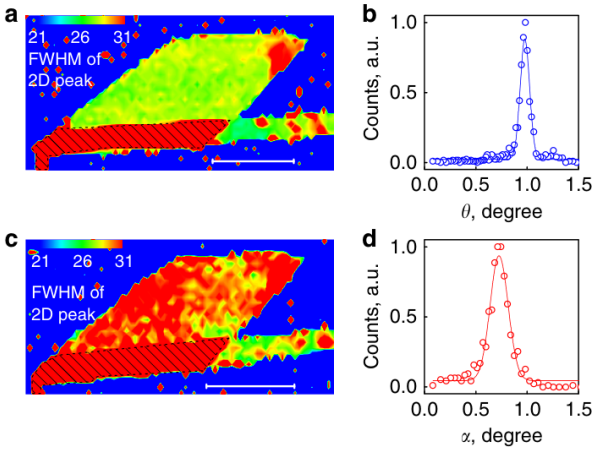

Figure 8: Raman spectroscopy before and after annealing. (adapted from [14])

8a, c: Maps of the FWHM of 2D Raman peak before and after self-rotation respectively.
8b, d: Bar charts of the misorientation angles calculated from a and respectively.

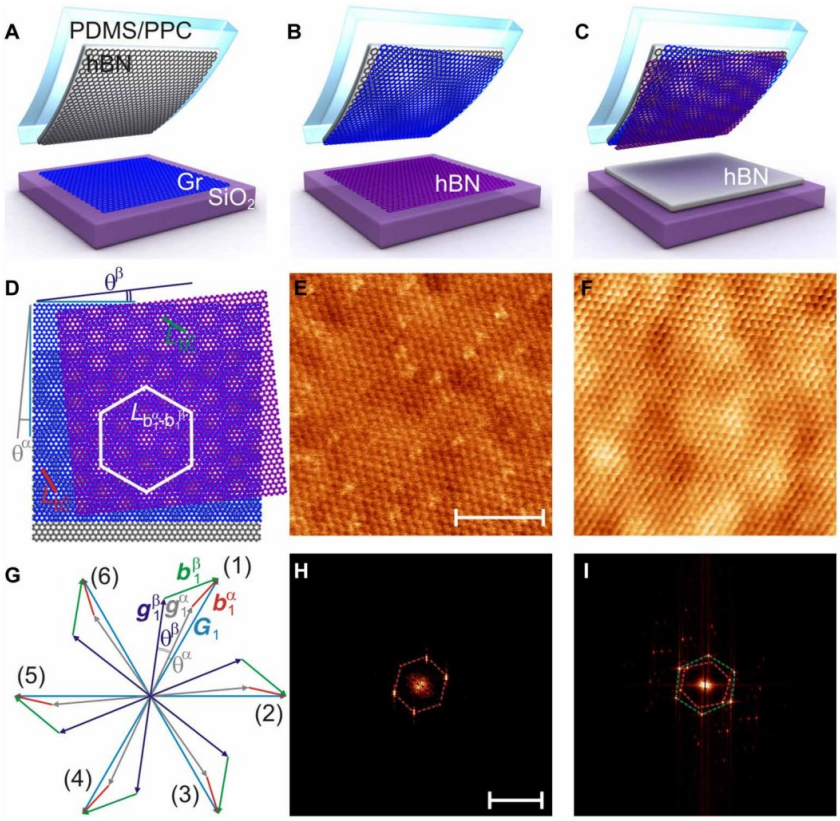

Figure 9: Experimental procedure and characterization of the two- and three-layer sample. (adapted from [15])

9a, b, c: Fabrication of the system.
9d: In the three-layer sample, two sub-moiré patterns and a super moiré pattern are illustrated directly.
9e: AFM image of the moiré pattern when graphene is attached to the base hBN forming a two-layer system. Only one periodicity is observed.

DOI: 10.54254/2753-8818/2025.23535

9f: AFM image of the moiré pattern when the last hBN is elevated forming a three-layer system. Two types of periodicities due to hBN layers are visible.

9g: Reciprocal space image of graphene's first Brillouin zone.

9h: Fourier transformation of the AFM image in 8e, exhibiting a single hexagonal pattern.

9i: Fourier transformation of the AFM image in 8f, exhibiting two sets of hexagonal patterns, represented by red and green hexagons respectively.

It is a natural tendency to expand the discussion to even multi-layer device and in the following part an hBN-graphene-hBN heterostructures is introduced, in which the graphene layer is encapsulated by the top and bottom hBN layer, presenting two moiré patterns that are referred to as super-moiré. [15] In fact, such a structure provides a more powerful controlling method in band reconstruction of graphene. A thin organic film is used as a Sellotape to lift the prepared hBN layer from the substrate and then brought it into contact with the graphene layer (Detailed procedure is depicted in Figure9a, b, c). AFM and Raman Spectroscopy are experimented on the bilayer system in order to check the alignment situation and results are showed in 9e, f, h, i. The AFM image exhibits clear hexagonal moiré pattern in accordance with the previous research and the same hexagonal symmetric points array of the Fourier transformation result is an additional confirmation. The similar operation is performed after the second layer of hBN is attached to the bilayer system and a double-aligned moiré pattern are presumably found. The two sets of hexagonal point arrays in the FT results further confirm the existence of two hexagonal moiré patterns.

3. Application

3.1. Photodetectors

Graphene is gifted with extremely high operation bandwidth because of its high carrier mobility which facilitates the fast extraction of carriers produced by photons, presenting itself as a promising new material photodetector. Given the saturated carrier velocity, its bandwidth considering the transit-time limitation is calculated to reach 1.5 THz while from the practical view, the time-constant of capacitive (RC) delay restrains the maximum bandwidth from exceeding 640 GHz [16], which is still far better than the existing semiconductor photodetectors like InGaAs and Ge with maximum bandwidth of 150 GHz and 80GHz respectively [5]. Several methods to improve graphene photodetectors' sensitivity and the pitiful effective absorption arears and thickness have been developed.

3.2. Energy storage

Energy storage is, at present, one of the most prevailing research fields connected with the idea of environmental preservation and the participation of graphene in the lithium-ion batteries is studied widely. High electric and thermal conductivity enable graphene to probably tackle the main hurdles encountered by the lithium-ion batteries i.e. low specific power density and the huge amount of heat generated within the battery system.

3.3. Bio-applications

A wide range of exceptional properties of graphene make it suitable for biological applications. For example, the large surface area and the chemical purity lay foundation for drug delivery. The lipophilicity of graphene also may be helpful in overcoming the challenge of membrane barrier penetration. In addition, graphene is able to be chemically functionalized for sensitive measurement application, which can detect various biological molecules including DNA [17].

DOI: 10.54254/2753-8818/2025.23535

4. Conclusion

Retracing the steps taken by former scientists, we have a glimpse at the physical configuration and various characteristics of graphene, including the quantum Hall effect and the commensurate-incommensurate transition. All of the exceptional properties represent graphene as an attractive candidate for the stage of wider future application and we review several recent developments of graphene relating photonic devices, energy storage and bio-applications. This bizarre two-dimensional is due to have a more powerful impact on the condensed matte research.

References

[1] *Novoselov, K. S., et al. "Two-dimensional atomic crystals." Proc Natl Acad Sci U S A 102.30(2005):10451-10453.*
[2] *Geim, A. K., and K. S. Novoselov, "The rise of graphene." Nature Materials 6(2009):11-19.*
[3] *Wallace, P. R., "The Band Theory of Graphite." Physical Review 71.9(1947):622-634.*
[4] *Novoselov, K S., et al. "Electric field effect in atomically thin carbon films." Science (New York, N.Y.) 306.5696(2004):666-9.*
[5] *Novoselov, K. S., et al. "A Roadmap for graphene." Nature 490.7419(2012):192-200.*
[6] *Yi, Min, and Z. Shen, "A review on mechanical exfoliation for the scalable production of graphene." Journal of Materials Chemistry A 3.22(2015):11700-11715.*
[7] *Jayasena, Buddhika, and S. Subbiah, "A novel mechanical cleavage method for synthesizing few-layer graphene." Nanoscale Research Letters 6.1(2011):95.*
[8] *Bae, S. K., et al. "Roll-to-Roll Production of 30-in. Graphene Films for Transparent Electrodes." Nature Nanotechnology 5(2011):574-578.*
[9] *Zhang, Yuanbo, et al. "Experimental observation of the quantum Hall effect and Berry's phase in graphene." Nature 438.7065(2005):201-204.*
[10] *Novoselov, K. S., et al. "Two-Dimensional Gas of Massless Dirac Fermions in Graphene." Nature (2005).*
[11] *Tang, Shujie, et al. "Precisely aligned graphene grown on hexagonal boron nitride by catalyst free chemical vapor deposition." Scientific Reports.*
[12] *Woods, C. R., et al. "Commensurate–incommensurate transition in graphene on hexagonal boron nitride." Nature Physics.*
[13] *Eckmann, Axel, et al. "Raman Fingerprint of Aligned Graphene/h-BN Superlattices." Nano Letters 13.11(201 3):5242-5246.*
[14] *Woods, C. R., et al. "Macroscopic self-reorientation of interacting two-dimensional crystals." Nature Commu nications.*
[15] *Wang, Zihao. "Composite super-moiré lattices in double aligned graphene heterostructures." APS March Meeting 2022 American Physical Society, 2022.*
[16] *Xia, Fengnian, et al. "Ultrafast graphene photodetector." Nature Nanotechnology (2009).*
[17] *Kuila, Tapas, et al. "Recent advances in graphene-based biosensors." Biosensors and Bioelectronics 26.12(2011):4637-4648.*